⌘ Author's Choice

Structural Basis for the Activity and Substrate Specificity of Fluoroacetyl-CoA Thioesterase FlK

Received for publication, January 23, 2010, and in revised form, April 8, 2010 Published, JBC Papers in Press, April 29, 2010, DOI 10.1074/jbc.M110.107177

Marcio V. B. Dias[‡1,2], Fanglu Huang[§2,3,4], Dimitri Y. Chirgadze[‡5], Manuela Tosin[§6], Dieter Spiteller[‡7], Emily F. V. Dry[§], Peter F. Leadlay[‡], Jonathan B. Spencer[§†], and Tom L. Blundell[‡]

From the [‡]Department of Biochemistry and [§]University Chemical Laboratory, University of Cambridge, Lensfield Road, Cambridge CB2 1EW, United Kingdom

The thioesterase FlK from the fluoroacetate-producing *Streptomyces cattleya* catalyzes the hydrolysis of fluoroacetyl-coenzyme A. This provides an effective self-defense mechanism, preventing any fluoroacetyl-coenzyme A formed from being further metabolized to 4-hydroxy-*trans*-aconitate, a lethal inhibitor of the tricarboxylic acid cycle. Remarkably, FlK does not accept acetyl-coenzyme A as a substrate. Crystal structure analysis shows that FlK forms a dimer, in which each subunit adopts a hot dog fold as observed for type II thioesterases. Unlike other type II thioesterases, which invariably utilize either an aspartate or a glutamate as catalytic base, we show by site-directed mutagenesis and crystallography that FlK employs a catalytic triad composed of Thr[42], His[76], and a water molecule, analogous to the Ser/Cys-His-acid triad of type I thioesterases. Structural comparison of FlK complexed with various substrate analogues suggests that the interaction between the fluorine of the substrate and the side chain of Arg[120] located opposite to the catalytic triad is essential for correct coordination of the substrate at the active site and therefore accounts for the substrate specificity.

In 1986, Sanada *et al.* (1) discovered that *Streptomyces cattleya* is able to produce fluoroacetate (FAc)[8] from fluoride. Attempts to elucidate the mechanism of this unusual transformation have led to the discovery of a fluorinase enzyme catalyzing the formation of 5′-fluoro-5′-deoxyadenosine from *S*-adenosyl-L-methionine and fluoride (2–6). We have cloned the fluorinase gene *flA* (5) and subsequently identified a gene cluster (*fl*) surrounding the fluorinase gene from *S. cattleya* (7). Characterization of the 5′-fluoro-5′-deoxyadenosine phosphorylase (3), the enzyme responsible for the second step of the FAc biosynthesis encoded by the *flB* gene located next to the *flA*, has confirmed the involvement of the *fl* gene cluster in the biosynthesis of FAc (7). In our efforts to further elucidate the functions of the *fl* gene cluster, the protein encoded by the *flK* gene located close to the 3′-end of the cluster was characterized as a thioesterase that cleaves fluoroacetyl-coenzyme A (FAcCoA) to produce FAc and CoA. It is noteworthy that acetyl-coenzyme A (AcCoA) is not hydrolyzed by FlK (7). Previous studies have shown that FAc can be used by AcCoA synthase to synthesize FAcCoA, and citrate synthase can catalyze formation of 2-fluorocitrate from FAcCoA and oxaloacetate (8). Lauble *et al.* (9) have shown that the (−)-*erythro* diastereomer of 2-fluorocitrate is further converted to 4-hydroxy-*trans*-aconitate, a lethal competitive inhibitor of aconitase, thereby blocking the tricarboxylic acid cycle. The presence of a FAcCoA-hydrolyzing enzyme that has no effect on the metabolically important intermediate AcCoA may therefore serve as a self-resistance mechanism for the FAc-producing *S. cattleya*.

FlK is homologous to many predicted thioesterases and hypothetical proteins according to protein-protein BLAST searches against a non-redundant protein sequence data base (7). However, none of these putative homologues has a defined function. Two groups of thioesterases have been identified, thioesterases I and thioesterases II, based on differences in their amino acid sequence, protein folds, and catalytic mechanisms. Type I thioesterases have evolved within the α/β-hydrolase fold superfamily and are usually present as a product-releasing domain of multidomain proteins, such as type I fatty acid synthases, polyketide synthases, and nonribosomal peptide synthases. Type I thioesterases use serine or cysteine as the catalytic residue (10, 11). Type II thioesterases are discrete proteins associated with activities of hydrolyzing short- or medium-chain acyl-CoAs and exist either as a homodimer of a single hot dog fold (12) or as a monomer comprising a duplicated hot dog fold (13). It has been shown that the active sites of type II thioesterase enzymes contain either a glutamate or an aspartate residue acting as a general base or nucleophile responsible for the catalytic function (14, 15), although the precise catalytic mechanism has remained controversial. FlK, a discrete protein catalyzing hydrolysis of a short-chain acyl-CoA (fluoroacetyl CoA), apparently belongs to the type II thioesterase family and

⌘ *Author's Choice*—Final version full access.

The atomic coordinates and structure factors (codes 3KX7, 3KX8, 3KV7, 3KV8, 3KVZ, 3KW1, 3KUV, 3KUW, 3KVU, and 3KVI) have been deposited in the Protein Data Bank, Research Collaboratory for Structural Bioinformatics, Rutgers University, New Brunswick, NJ (http://www.rcsb.org/).

† This work is dedicated to the memory of Dr. J. B. Spencer, who passed away on April 6, 2008.

[1] Recipient of a postdoctoral fellowship from the Conselho Nacional de Desenvolvimento Cientifico e Tecnológico.

[2] Both authors contributed equally to this work.

[3] Supported by Biotechnology and Biological Sciences Research Council Grant BBSB13357.

[4] To whom correspondence should be addressed. Tel.: 44-1223-336710; Fax: 44-1223-336362; E-mail: fh223@cam.ac.uk.

[5] Supported by Wellcome Trust Programme Grant 079281/Z/06/Z.

[6] Recipient of the Herchel Smith Fund Fellowship.

[7] Present address: Dept. of Bioorganic Chemistry, Max Planck Institute for Chemical Ecology, Hans-Knöll-Strasse 8, D-07745 Jena, Germany.

[8] The abbreviations used are: FAc, fluoroacetate; Ac, acetate; AcCoA, acetyl-coenzyme A; FAcCoA, fluoroacetyl-coenzyme A; FAcCPan, fluoroacetyl carba(dethia)-pantetheine; FAcOPan, fluoroacetyl oxa(dethia)-pantetheine; CHES, 2-(cyclohexylamino)ethanesulfonic acid; WtFlK, wild type FlK; SeMet, selenomethionine.

is therefore expected to have a carboxylic side chain at the active site. Protein sequence alignment analysis has revealed that nine amino acid residues in FlK (Gly^{8}, Thr^{42}, Glu^{50}, Leu^{61}, Gly^{69}, His^{76}, Ala^{78}, Gly^{83}, and Gly^{116}) are all conserved in homologues that have a similar protein size to FlK (ranging from 127 to 180 amino acids). The presence of Thr^{42} and His^{76} together with Glu^{50} among the conserved residues led us to speculate that FlK may employ a variation of the classical catalytic triad-type mechanism with Thr^{42} (instead of a Ser or a Cys), His^{76}, and Glu^{50} (instead of an Asp). His^{76} would then serve as a base to deprotonate Thr^{42}. The deprotonated Thr^{42}-$O_{\gamma 1}$ is proposed to act as a nucleophile attacking the fluoroacetyl carbonyl carbon of FAcCoA to initiate the hydrolysis reaction and the carboxylic side chain of Glu^{50} to neutralize the charge developed on the His^{76} side chain during the transition state of the reaction by hydrogen bonding with the imidazole nitrogen of His^{76} (7). Although a hydroxyl derived from threonine rather than from a serine residue has been found to act as the catalytic nucleophile in some proteinases, including the individual activities of the proteosome (16), to the best of our knowledge, no functionally characterized thioesterase has been reported to use threonine in this way.

We have carried out site-directed mutagenesis targeting the putative catalytic residues and defined structures by x-ray crystallography of the wild type and mutant FlK proteins both with and without bound analogues of FAcCoA. Our studies provide insights into the catalytic mechanism of FlK and the high substrate specificity of FlK for FAcCoA over the closely related AcCoA.

EXPERIMENTAL PROCEDURES

Cells, Reagents, and Equipment—All oligonucleotide primers were synthesized by MWG-Biotech. Restriction enzymes were purchased from New England Biolabs, T4 DNA ligase was from Fermentas Life Sciences, and cloned Pfu DNA polymerases were from Stratagene. The following reagents were purchased from Sigma: AcCoA, 5,5′-dithio-bis(2-nitrobenzoic acid) (Ellman's reagent), CHES, ethylene glycol, polyethylene glycol 4000, polyethylene glycol monomethyl ether 2000, potassium chloride (KCl), L-selenomethionine (L-SeMet), trisodium citrate, Tris, sodium acetate, and sodium fluoroacetate. Amino acids used for cell cultures were from DUCHEFA Biochemie. FAcCoA was synthesized as described previously (7). An ÅKTA FPLC system and a HiLoad Superdex S200 column (16 × 60 cm) (GE Healthcare) were used for gel filtration purification of proteins. The protein concentration was determined using the Bradford method (Sigma). DNA sequencing was performed in the Department of Biochemistry DNA Sequencing Facility (University of Cambridge) on an Applied Biosystems 3730xl DNA analyzer. *Escherichia coli* NovaBlue or DH10B cells were used for cloning, and *E. coli* Rosetta™ (DE3)pLysS cells were used for protein expression.

Cloning of FlK and Mutants—The cloning of the recombinant His-tagged wild-type FlK (WtFlK) in pET28a(+) (Novagen) was described in our previous study (7). Mutants of FlK each containing a single amino acid mutation were created by PCR using the WtFlK-expressing plasmid as a template. For each mutant, two PCR amplifications were carried out using two primer pairs: T7-27/3′-5′ primers for PCR-1 and T7T-27/5′-3′ primers for PCR-2. The T7–27 primer (5′-TAATACGACTCACTATAGGGGAATTGT-3′) and T7T-27 primer (5′-GCTAGTTATTGCTCAG CGGTGGCAGCA-3′) hybridize, respectively, to the upstream or downstream regions of the multicloning site in pET28a(+). Mutations were created in either the 3′-5′ primer or the 5′-3′ primer or both, depending on the specific design for each individual mutant.

PCR was carried out using cloned *Pfu* DNA polymerase (Stratagene) with 25 cycles of denaturation at 94 °C for 1 min, annealing at 55 °C for 1 min, and extension at 72 °C for 1 min plus a final extension at 72 °C for 10 min. The resulting PCR products were digested with appropriate restriction enzymes, purified by gel extraction (Qiagen), and inserted into pET28a(+) vector between the NdeI and BamHI sites. The inserts of the recombinant plasmids were verified by DNA sequencing. Constructs with the correct inserts were introduced into *E. coli* Rosetta™ (DE3)pLysS competent cells (Novagen) for protein expression.

Expression and Purification of FlK and FlK Mutants—An overnight culture (10 ml) from a single colony harboring the desired plasmid was used for inoculation of 1 liter of fresh LB medium containing kanamycin (50 μg/ml). The culture was incubated at 37 °C, 250 rpm until A_{600} = 0.5–0.8 was reached. Overexpression of the proteins was induced by 0.2–0.3 mM isopropyl 1-thio-β-D-galactopyranoside overnight at 16 °C with shaking at 220 rpm before being harvested by centrifugation. For incorporation of L-SeMet into FlK, 1 liter of fresh medium containing 6 g of Na_2HPO_4, 3 g of KH_2PO_4, 1 g of NH_4Cl, 1 g of NH_4Cl, 0.5 g of NaCl, 1 mM $MgSO_4$, 4 g of glucose, 0.5 mg of thiamine vitamin B1, and 50 mg of kanamycin was inoculated with cells from a 10-ml overnight culture and incubated at 37 °C with shaking at 250 rpm. When the cell density reached A_{600} = 0.3–0.5, a mixture of L-lysine (100 mg), L-phenylalanine (100 mg), L-threonine (100 mg), L-leucine (50 mg), L-isoleucine (50 mg), L-valine (50 mg), and L-SeMet (50 mg) was added into the culture, and incubation was continued for 30 min at 37 °C. Isopropyl 1-thio-β-D-galactopyranoside was then added to a final concentration of 1 mM to induce protein overexpression overnight at 16 °C, 200 rpm. The cells were broken by sonication for 4 min (1 s on, 10 s off) to release overexpressed recombinant protein. The supernatant of the cell lysate was applied to a His-Bind® column (Novagen) charged with Co^{2+} ions. Nonspecific proteins were removed by washing the column with washing buffer (0.5 M NaCl, 40 mM imidazole, 20 mM Tris-HCl, pH 7.9), and the recombinant protein was eluted with elution buffer (0.5 M NaCl, 200 mM imidazole, 20 mM Tris-HCl, pH 7.9). The buffer containing the purified proteins was exchanged with a buffer containing 100 mM KCl and 20 mM Tris-HCl, pH 7.5, and concentrated at 4 °C to a total volume of 1–2 ml. The His tag of the proteins was removed by thrombin (restriction grade; Novagen) digestion at room temperature overnight. The tag-free proteins were further purified by gel filtration on an ÄKTA Explorer FPLC system using a HiLoad™ 16/60 Superdex™ 200 Prep Grade column and a mobile phase containing 100 mM KCl and 20 mM Tris-HCl, pH 7.5. The purity of the proteins was checked by SDS-PAGE. The protein masses were confirmed by liquid chromatography-electrospray ionization-mass spec-

trometry on a 2.0 × 250-mm Jupiter 5-μm C4 column (Phenomenex) using a Finnigan LCQ (Thermo Finnigan) coupled with an HP1100 high pressure liquid chromatography system (Agilent) with a flow rate of 0.2 ml/min and the following mobile phase gradient: 0–5 min, 35–45% B; 5–25 min, 45–75% B; 25–30 min, 75–95% B (buffer A: 0.1% trifluoroacetic acid in H_2O; buffer B: 0.1% trifluoroacetic acid in acetonitrile).

Enzymatic Assays—The thioesterase activity of FlK and its mutants on FAcCoA was measured by monitoring spectrophotometrically the increase in absorbance at 412 nm due to the reaction of released CoASH with 5,5′-dithio-bis(2-nitrobenzoic acid with a CARY 100 Bio UV-visible spectrophotometer (Varian) as described previously (7). All assays were performed at 25 °C in a total volume of 0.5 ml in a spectrophotometer cuvette with a 1-cm light path.

Preparation of Fluoroacetyl Carba(dethia)-pantetheine and Fluoroacetyl Oxa(dethia)-pantetheine—To prepare fluoroacetyl carba(dethia)-pantetheine (FAcCPan), monofluorination of (*O*,*O*′-diacetyl)-malonyl carba(dethia)-pantetheine methylester with Selecfluor™ was carried out, followed by base-catalyzed loss of the protecting groups and concomitant deprotection and decarboxylation of the malonyl moiety. Fluoroacetyl oxa(dethia)-pantetheine (FAcOPan) was obtained from 1-ethyl-3-(3-dimethylaminopropyl) carbodiimide coupling of *O*,*O*′-isopropylidene-oxa(dethia)-pantetheine with sodium fluoroacetate, followed by acetal deprotection with Dowex 50-X8-400.

Crystallization of SeMet FlK in the Apo-form—The crystallization trials with the SeMet FlK protein at a concentration of 20 mg/ml in 50 mM Tris-HCl and 100 mM KCl, pH 7.5, were carried out using a Cartesian HONEYBEE™ 81 crystallization robot (Genomic Solutions), and protein crystallization was screened using the crystallization conditions from SM1 (Nextal) and the Classics (Qiagen) crystallization solution kits. To each reservoir of 96-well CrystalQuick crystallization plates with square sitting drop position (Molecular Dimensions) were added 100 μl of the crystallization solution and 100 nl of protein solution. The best crystals appeared after approximately 1 week in 0.1 M Tris, pH 7.5, and 20% polyethylene glycol monomethyl ether 2000.

Crystallization of Wild-type FlK (WtFlK) and Its Mutants (T42SFlK and T42AFlK) in Complex with Acetate (Ac) and FAc—Initially, crystallization trials were carried out using hanging drop vapor diffusion at 293 K. The protein at 10 mg/ml in 50 mM Tris-HCl buffer, pH 7.5, containing 100 mM KCl was screened against mother liquor solutions from the Classics suite (Qiagen) and kept at 20 °C. The initial crystals were obtained in 30% polyethylene glycol 4000, 0.1 M sodium acetate, and 0.1 M Tris-HCl, pH 7.0. After optimization, the best crystals were obtained with protein at 5 mg/ml in the same crystallization condition. The drops comprised 1 μl of protein solution and 1 μl of crystallization solution, and the crystals appeared after 3 or 4 days. To crystallize the FlK in complex with FAc, the sodium acetate present in the crystallization solution was replaced by 0.2 M sodium fluoroacetate. The crystals for both complexes were flash-frozen in liquid nitrogen to perform the data collection after soaking in cryoprotectant solution composed of 25–30% ethylene glycol and 75–70% well solution. Both mutants (T42SFlK and T42AFlK) and WtFlK were crystallized under the same conditions.

Crystallization of T42SFlK in Complex with AcCoA—After ~6 months, crystals of T42SFlK·AcCoA complex grew in conditions similar to those for the WtFlK·Ac complex except where the acetate was replaced with 20 mM AcCoA.

Crystallization of WtFlK in Complex with Analogues of Fluoroacetyl Pantetheine—The protein was incubated with 5 mM either FAcCPan or FAcOPan. Initial trials were carried out using a Cartesian HONEYBEE™ 81 crystallization robot (Genomic Solutions), and the protein was screened using the crystallization conditions from SM1 (Nextal), Classics, pHclear, and pHclear II (Qiagen) crystallization solution kits. In each reservoir of the 96-well CrystalQuick crystallization plate with square sitting drop position (Molecular Dimensions), 100 μl of the crystallization solution was added. The drops contained 100 nl of the reservoir solution and 100 nl of protein solution at 10 mg/ml in 50 mM Tris-HCl and 100 mM KCl, pH 7.5. The best hits without acetate appeared in a condition that comprised 100 mM CHES, pH 9.5, and 1 M trisodium citrate. After optimization, the best crystals were obtained in a condition containing 100 mM CHES, pH 9.5, and 0.8 M trisodium citrate with a protein concentration of 10 mg/ml in the presence of 10 mM FAcCPan or FAcOPan.

Data Collection and Structure Determination—Data for apoform WtFlK and SeMet FlK were collected at beamline ID14.4, European Synchrotron Radiation Facility (Grenoble, France). The data sets were processed using DENZO and SCALEPACK (version 1.97) (17). The data were truncated and converted to structure factors using TRUNCATE (18) from the CCP4 suite (19). X-ray data for complexes of WtFlK·FAc, T42AFlK·FAc, T42SFlK·AcCoA, WtFlK·FAcCPan, and WtFlK·FAcOPan were collected at the Swiss Light Source, and the WtFlK·Ac, T42SFlK·Ac, and T42SFlK·FAc were collected at the European Synchrotron Radiation Facility. The data sets were processed using the program Mosflm (20) and scaled by SCALA (21). The structure of SeMet FlK in its apo-form was solved using single-wavelength anomalous diffraction and the Phenix program (22), and the other structures were solved by molecular replacement using the apo-structure as probe search in the program AMoRe (23) in the CCP4 suite (19). The refinement was carried out using the program REFMAC 5.2 (24). Visual inspection and water addition were performed using XtalView/xfit (25) and Coot (26). The quality of the model was assessed using PROCHECK (27). The figures were made using PyMOL (28).

RESULTS

Site-directed Mutagenesis—To investigate the reaction mechanism of FlK, mutants of FlK were created at residues Thr^{42}, Glu^{50}, and His^{76}, candidates for the catalytic triad in the FlK protein. To assess the involvement of these residues in the catalytic mechanism, the activities of the mutants were assayed and compared with that of WtFlK. Four mutants of the FlK protein carrying single amino acid mutations (T42S, T42A, E50A, and H76D, respectively) were cloned in pET28a(+) and overexpressed in *E. coli* Rosetta™ (DE3)pLysS cells as His-tagged proteins. All proteins were purified by Co^{2+}-charged

TABLE 1

Comparison of wild-type and mutant FlK

Enzyme reactions were carried out using FAcCoA as the substrate. Errors quoted represent the S.E. of curve fitting (Lineweaver-Burk plot). Each data point is the average of four (WtFlK), three (T42SFlK), or two E50AFlK measurements.

Protein	Soluble protein	k_{cat} [a]	K_m	k_{cat}/K_m [b]	FAcCoA concentration above which substrate inhibition was observed
	mg/liter	s^{-1}	μM	$m_M{}^{-1}\,s^{-1}$	μM
WtFlK	~10–12	0.044 ± 0.001	30 ± 1.3	1.47 ± 0.10	
T42SFlK	~10–12	0.409 ± 0.159	15 ± 1.2	27.3 ± 12.8	12
T42AFlK	~2				
E50AFlK	~2	0.111 ± 0.041	206 ± 67	0.54 ± 0.37	19

[a] The units are number of CoA released/s/enzyme molecule.
[b] The error values given for k_{cat}/K_m are calculated from the sum of the relative errors on values in the numerator and denominator.

His-Bind resin (Novagen) followed by gel filtration. Both WtFlK and T42SFlK were expressed as soluble proteins with a yield of over 10 mg from 1 liter of culture. T42AFlK and E50AFlK mutants yielded only 2 mg of soluble enzyme/liter of culture, although their expression levels were comparable with those of WtFlK and T42SFlK. During storage at 4 °C T42SFlK and T42AFlK also showed a much higher tendency to aggregate than WtFlK. The recombinant H76DFlK protein expressed in *E. coli* was completely insoluble, so it was not used for further studies. All of the mutations seemed have disturbed protein folding, with the H76D mutant being the most affected. The molecular weights of the purified proteins were determined by liquid chromatography-electrospray ionization-mass spectrometry. Retention times on gel filtration through a Superdex S200 column indicate that purified WtFlK and the T42AFlK, T42SFlK, and E50AFlK mutants are all dimers.

The enzymatic characterization of WtFlK using FAcCoA as substrate has been reported previously (7). The present study demonstrated that replacing the Thr42 with Ala[42] in FlK abolishes the enzyme activity, supporting our hypothesis that the Thr[42]-$O_{\gamma 1}$ may act as the catalytic nucleophile that attacks the carbonyl thioester carbon of FAcCoA to initiate the hydrolysis reaction. Not surprisingly, T42SFlK is still able to hydrolyze FAcCoA with a k_{cat}/K_m value of 27.3 $m_M{}^{-1}\,s^{-1}$, which is about 19 times higher than that for WtFlK (1.47 $m_M{}^{-1}\,s^{-1}$), and a relatively smaller K_m value (15 μM, 50% lower than that for WtFlK (30 μM)). It is noteworthy that T42SFlK activity was inhibited at a substrate concentration above 12 μM. These results suggest that the Ser[42]-Oγ in T42SFlK is able to carry out the nucleophilic attack and that the absence of the Thr[42]-Cγ in the T42S mutant may have led to decreased ability to ensure correct substrate binding, resulting in the substrate inhibition. The k_{cat}/K_m value of E50AFlK (0.54 $m_M{}^{-1}\,s^{-1}$) is only 37% of that for WtFlK, whereas the K_m (206 μM) is much higher than that for WtFlK. E50AFlK also exhibited substrate inhibition when the FAcCoA concentration was above 19 μM, suggesting that Glu[50] plays an important role in substrate recognition (Table 1).

FlK Crystal Structure Determination—In order to understand the catalytic mechanism of FlK, in particular how FlK distinguishes between FAcCoA and the structurally very similar AcCoA, 10 crystal structures of WtFlK, T42SFlK, and T42AFlK with or without various ligands were determined. The WtFlK structures were solved in the apo-form and in complex with either the substrate analogue AcCoA or the substrate fragment analogues FAcCPan and FAcOPan, the product FAc, or the product analogue Ac. Although attempts to crystallize T42S and T42A mutants in their apo-forms failed, crystals of T42SFlK in complex with Ac, FAc, or AcCoA and T42AFlK with bound FAc were obtained, and their structures were solved.

Overall Fold and Oligomeric Association of FlK—The crystals of FlK diffracted at resolutions between 2.35 and 1.5 Å and belong to space group C2 or $P2_1$ with two, four, or eight FlK molecules in the asymmetric unit, depending on the nature of the complex. Those complexes that crystallized in C2 (WtFlK·Ac, WtFlK·FAc, T42SFlK·Ac, T42SFlK·FAc, and T42AFlK·FAc) have a dimer in the asymmetric unit with a local 2-fold symmetry axis. The crystals in $P2_1$ have either dimers (two in T42SFlK·AcCoA and apo-SeMet WtFlK) in the asymmetric unit, also with local 2-fold symmetry, or two tetramers (WtFlK·FAcCPan and WtFlK·FAcOPan) with orthogonal 2-fold axes giving 222 pseudosymmetry (Fig. 1, *A* and *B*). Operation of the crystallographic 2-fold axis on the dimers in the asymmetric unit in space group C2 generates a tetramer, identical to that observed in the WtFlK·FAcPan or WtFlK·FAcOPan crystal structures. The observation that these crystal structures contain discrete tetramers suggests that the protein may have dimer-tetramer equilibrium in solution in which tetramers predominate at high concentrations.

The protomer of FlK has a hot dog fold that comprises a five-strand antiparallel β-sheet (the bun) wrapping around a central α-helix (the sausage) (Fig. 1*A*). The hot dog fold was first observed for the structure of β-hydroxydecanoyl thiol ester dehydratase (12). A diverse range of enzymes with distinct catalytic activities has been found to have this fold. Thioesterases are important members of the hot dog superfamily and include 4-hydroxybenzoyl-CoA thioesterases from *Pseudomonas* sp. CBS-3 (29) and from *Arthrobacter* sp. SU (30), *Escherichia coli* thioesterases II (13), and acyl-CoA thioesterases YciA from *Hemophilus influenzae* (HI0827) (31). Despite the conserved hot dog fold, these thioesterases share a very low degree of identity at amino acid sequence level. The FlK asymmetric unit contains a dimer with pseudosymmetry about a 2-fold axis as observed previously in the structure of 4-hydroxybenzoyl-CoA thioesterase from *Pseudomonas* sp. (29). and (*R*)-specific enoyl-CoA hydratase from *Aeromonas caviae* (32). Most other thioesterases with the hot dog fold form tetramers, although hexameric structures have also been observed (31, 33). The main contacts between the two protomers in the FlK dimer are through strand 2 (residues 70–76) of the two protomers. The β-strands of the two protomers form together a 10-strand

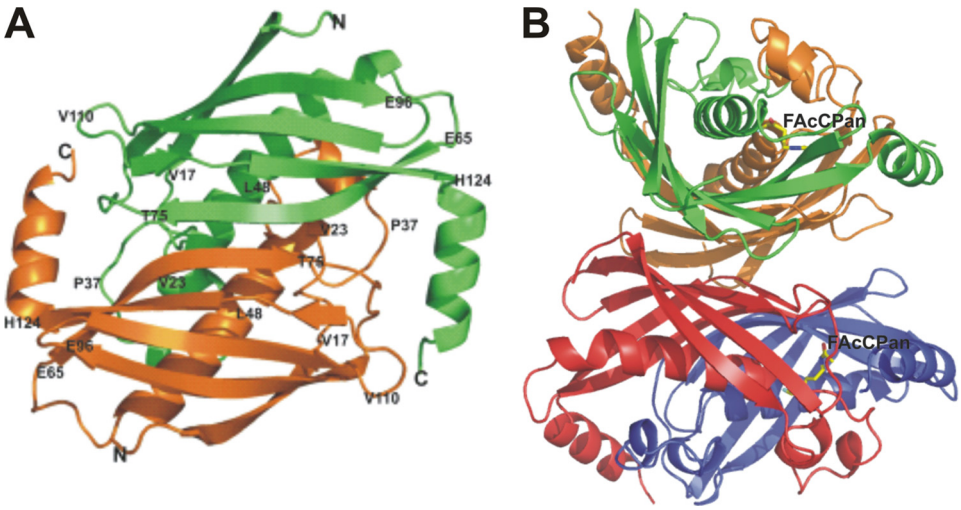

FIGURE 1. **Overall structure of FlK depicted in a schematic representation.** *A*, structure of WtFlK dimer. The two protomers of the dimer are shown in *green* and *orange*, respectively. *B*, tetrameric structure (dimer of dimers) of WtFlK in complex with the substrate analogue FAcCPan. The FAcCPan molecule is shown as *sticks*. The two protomers of the dimer on the top are indicated in *green* and *orange*, respectively. A *red/blue* color scheme is used for the dimer at the bottom.

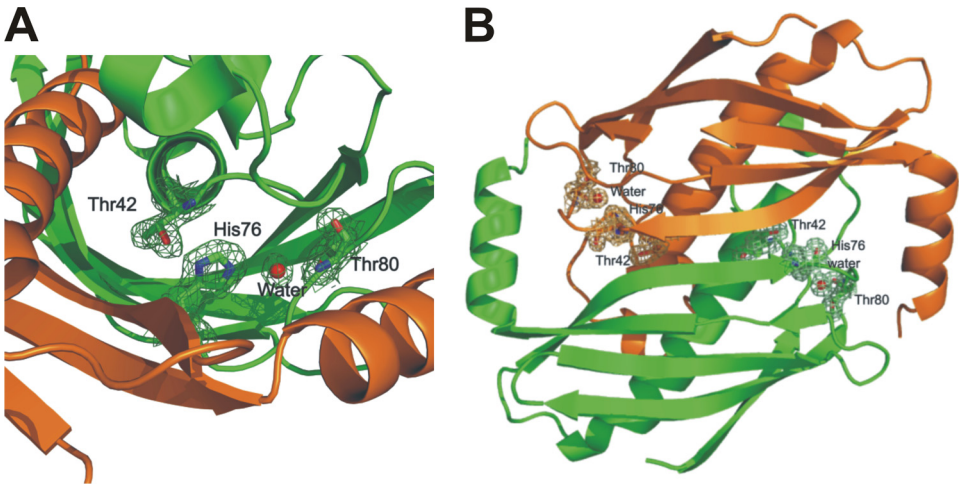

FIGURE 2. **Catalytic center of FlK.** *A*, the catalytic triad of FlK is composed of Thr^{42}, His^{76} (shown as *sticks*), and a conserved water molecule (Wat) (shown as a *sphere*). *Green* and *orange colors* indicate the two protomers of the dimer, respectively. *B*, the catalytic triad is located at the dimer interface. The electron density map used was $2F_o - 2F_c$.

protomer, suggesting strong interactions between them. These observations have led us to assume that the minimal active unit of FlK is a dimer.

The tetrameric structure observed for WtFlK·FAcCPan is formed by a dimer of dimers with pseudo 222 symmetry (Fig. 1*B*). The main interaction regions are the 10-strand β-sheets present in the dimers, which are positioned back to back. Non-polar interactions predominate, but additionally there are some water-mediated hydrogen bonds. Similar tetramers have been observed in other thioesterases (13, 30, 34, 35). The contact area between two dimers is ~3300 Å^2, corresponding to about 30% of the total solvent-accessible area of each dimer, further suggesting the possibility of an equilibrium between dimers and tetramer in solution.

The Active Site—Consistent with the results of the site-directed mutagenesis of FlK described above, the crystal structure of apo-form WtFlK shows that side chains of the candidate catalytic residues Thr^{42} and His^{76} in one protomer and that of Glu^{50} from the adjacent protomer cluster between the dimer interface into the region between the "bun" and the "sausage" (Fig. 2, *A* and *B*). As expected, the $O_{\gamma 1}$ of Thr^{42} and the $N_{\delta 1}$ of His^{76} are within hydrogen bonding distance (2.74 Å). To our surprise, we observed that the carboxylic group of Glu^{50} is located on the opposite side of Thr^{42}, where it cannot have any direct contact with His^{76}. However, a water molecule (Wat^1) is in a perfect position to form a hydrogen bond with the $N_{\delta 2}$ of His^{76} (2.79 Å). This water molecule is conserved in the crystal structures of wild-type and mutant FlK with or without bound ligands. Although this observation was unexpected, it is in good agreement with our site-directed mutagenesis results. A water molecule replacing the acidic residue in this type of catalytic triad was also found in the HAV-3C gene product, an α-chymotrypsin-like protease produced by the hepatitis A picornavirus (36). The Thr^{42}-His^{76}-Wat^1 network is further stabilized by a hydrogen bond between Wat^1 and Thr^{80} side chain hydroxyl and another conserved water molecule (Wat^2) that also forms a hydrogen bond with the Phe^{40}-N. Around the His^{76}-Wat^1-Thr^{80}/Wat^2 network, the side chains from Val^{39}, Phe^{40}, Ala^{78}, Ala^{79}, and Ile^{113} form a hydrophobic shield, protecting the network

β-sheet with the putative active site at the interface between the protomers. A disulfide bond formed by their respective Cys^{73} residues covalently connects the two subunits. Wrapping around the disulfide bond are the Ile^{72} and the Val^{74} from both protomers with their side chains within hydrophobic interaction distance of each other. The $C_{\gamma 2}$ of the putative catalytic Thr^{42} also makes a hydrophobic contact with Ile^{72}-$C_{\gamma 2}$ of the partner protomer. All of these interactions contribute to bringing the two protomers together. Furthermore, there are two salt bridges formed between the two protomers; the Lys^{21}-N_ζ interacts with the Glu^{29}-$O_{\epsilon 2}$, and Lys^{135}-N_ζ interacts with the carboxyl $O_{\delta 2}$ groups of Asp^{111} and Asp^{108} in the partner protomer. Hydrogen bonds formed by Ser^{30}-O_γ and Glu^{32}-$O_{\epsilon 1}$ with Trp^{51}-$N_{\epsilon 1}$, Gly^{43}-N with Glu^{50}-$O_{\epsilon 2}$ through a water molecule, and Tyr^{27}-OH with Phe^{44}-O also serve to stabilize the FlK dimer. The contact area between two protomers is ~1750 Å^2, corresponding to 30% of the accessible surface area of each

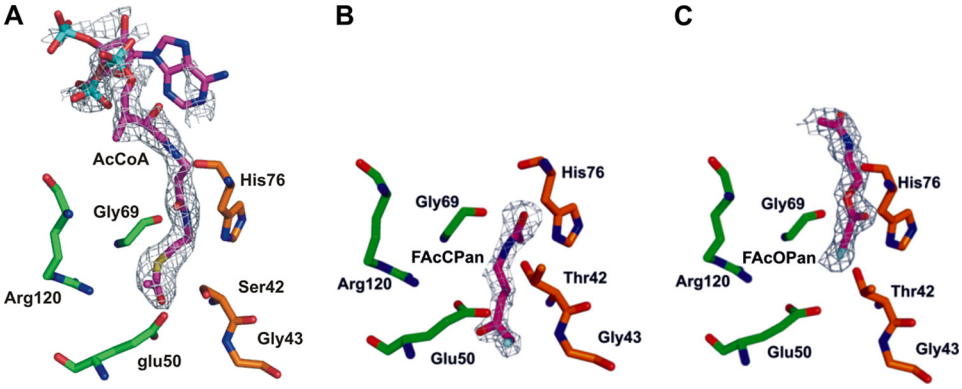

FIGURE 3. **Active sites of ligand-bound FlK with $2F_o - 2F_c$ electron density map for T42SFlK·AcCoA (*A*), WtFlK·FAcCPan (*B*), and WtFlK·FAcOPan (*C*).** The molecules of AcCoA, FAcCPan, and FAcOPan are all shown in a *deep purple color*. *Green* and *orange colors* indicate residues from the two protomers of the dimer.

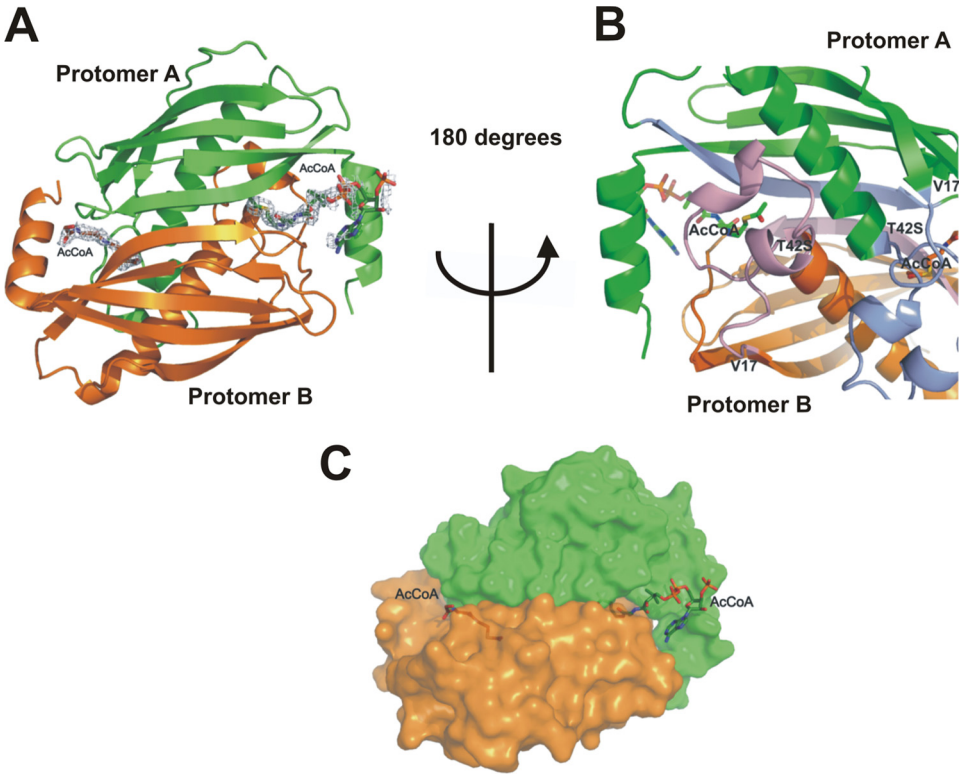

FIGURE 4. **Overall structure of T42SFlK in complex with AcCoA.** The two protomers of the T42SFlK dimer are represented in *green* and *orange colors*, respectively. *A*, $2F_o - 2F_c$ electron density map shows that AcCoA is bound between two protomers of the active FlK dimer. *B*, AcCoA is sandwiched between the long β-sheet and two small α-helices formed by residues 17–42. The long β-sheet and two small α-helices of protomer A and B are shown in *light blue* and *light purple*, respectively. *C*, representation of the molecular surface shows that only the acetyl and β-mercaptoethylamine moieties from AcCoA are buried in the active site of the protein.

from attack by solvent molecules. Based on our structural evidence, we now propose that the catalytic triad in FlK comprises Thr^{42}-His^{76}-water (Fig. 2*A*), located at the interface between two protomers with two active sites in each FlK dimer (Fig. 2*B*).

Substrate Binding Pocket—Although attempts to co-crystallize FlK with FAcCoA, CoA, or pantothenic acid failed, we successfully obtained crystals of T42SFlK with bound AcCoA and WtFlK in complex with two analogues of fluoroacetyl-pantetheine, FAcCPan, and FAcOPan. The sulfur atom of the thioester is replaced by a methylene in FAcCPan and by an oxygen atom in FAcOPan (Fig. 3). Comparison of the electron density maps of the crystals obtained from co-crystallization of WtFlK with FAc and CoA indicates that only FAc was bound. Comparisons of the structure of WtFlK without bound ligand with those of WtFlK·FAcCPan, WtFlK·FAcOPan, and T42SFlK·AcCoA have provided interesting insights into the structural basis of substrate recognition by FlK.

In the ligand-free WtFlK crystal structure, three well conserved water molecules (designated Wat^3, Wat^4, and Wat^5) mediate a hydrogen bonding network linking Thr^{42} and Gly^{43} in one protomer to Glu^{50}, Arg^{120}, and Gly^{69} in the neighboring protomer; Wat^3 links the Gly^{43}-N with the Glu^{50}-$O_{\epsilon 2}$, and Wat^4 and Wat^5 are within hydrogen bonding distance of each other and of the Thr^{42}-N and Gly^{69}-N, respectively. The Arg^{120}-NH_1 joins the network by salt bridging with Glu^{50}-$O_{\epsilon 1}$ and hydrogen bonding with Wat^5. Converting Arg^{120} to Ala^{120} yielded completely insoluble protein, as did converting Glu^{50} to Ala^{50}, suggesting the importance of these interactions in maintaining the correct protein folding and/or the correct architecture of the active site cavity.

In the T42SFlK·AcCoA complex, the AcCoA is sandwiched between the long β-sheet and residues 17–42 that form two small α-helices (Fig. 4*B*). However, only the acetyl and β-mercaptoethylamine moieties from acetyl-CoA are buried in the protein, whereas the pantothenic acid and the 3′-phosphoryl-ADP are exposed to solvent, allowing considerable flexibility (Fig. 4, *A* and *B*). Three of the four protomers present in the asymmetric unit have a bound AcCoA, and in one of them, it was possible to fit the complete molecule, despite the poor electron density for the 3′-phosphoryl-ADP moiety, possibly due to the high flexibility in the solvent. The overall structure of FlK does not change significantly as a result of the T42S point mutation and the binding of AcCoA, but the AcCoA has forced Wat^4 and Wat^5 out of the active site cavity. The acetyl methyl group of the AcCoA occupies the position of Wat^5, and the thioester carbonyl oxygen interacts via a hydrogen bond to Ser^{42}-N. The orientations of the three bound AcCoA molecules at the active site are significantly different, reflecting a dynamic AcCoA-FlK interaction process and the flexibility of the substrate binding

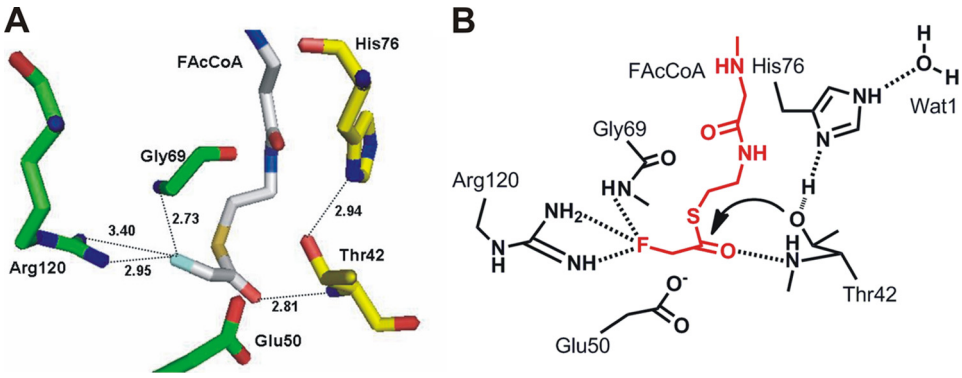

FIGURE 5. **Proposed FAcCoA coordination at the active site of FlK.** *A*, a stick model with FAcCoA shown in *silver* and residues from the two protomers represented in *yellow* and *green colors*, respectively. *B*, a scheme with FAcCoA (*red*) and active site residues (*black*). Hydrogen bonding interactions are denoted by *dotted lines* with distance in Å.

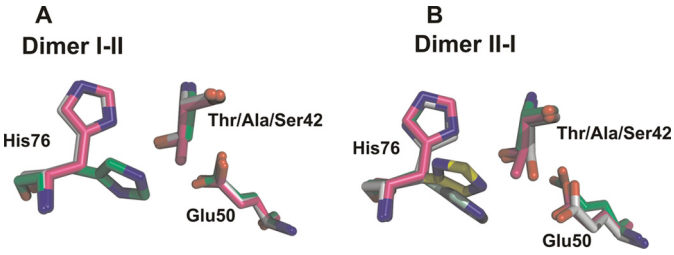

FIGURE 6. **Structural differences observed in the catalytic site of FlK due to different mutations of Thr^{42}.** The active site residues Thr^{42}, His^{76}, and Glu^{50} of WtFlK are superimposed with their counterpart residues in T42AFlK and T42SFlK. *A*, Thr/Ala/Ser^{42} and His^{76} from protomer I and the Glu^{50} from protomer II; *B*, Thr/Ala/Ser^{42} and His^{76} from protomer II and the Glu^{50} from protomer I. *Pink*, WtFlK; *green*, T42AFlK; *white*, T42SFlK. The alternative conformations of His^{76} in T42A (*pale green*) and in T42S (*yellow*) are indicated.

site. The acetyl carbonyl carbons of the three bound AcCoA molecules are all in the wrong orientation with respect to O_γ of Ser^{42} to allow nucleophilic attack. This explains the inability of FlK to hydrolyze AcCoA and implies that the presence of the fluorine in FAcCoA is crucial for substrate recognition.

The positions of FAcCPan and FAcOPan in WtFlK differ significantly from that of AcCoA in the T42SFlK·AcCoA structure. Compared with the bound AcCoA, the bound FAcCPan is buried deeper in the active site, and the FAcOPan is located closer to the entrance of the tunnel (Fig. 3*B*). In a way that resembles the binding of AcCoA in T42SFlK, the carbonyl carbons of both FAcCPan and FAcOPan in WtFlK are in the wrong position and are even further away (3.88, 3.94, and 5.26 Å, respectively) from the $O_\gamma$of Thr^{42}. Furthermore, the binding coordinates of the same molecule also vary in different FlK dimers, suggesting that the presence of the nucleotide part of the CoA moiety is required for the correct overall engagement of the substrate at the substrate-binding site.

In all of the FAc or Ac-bound FlK complexes, more than one molecule of FAc or Ac is bound in the large cavity of each active site. This may be a consequence of the high ligand concentrations (0.2 M) used in the crystallization solution and of the absence of the substrate. Interestingly but not surprisingly, at each active site, there is always one ligand situated at a position to where either the acetyl group of the AcCoA or the equivalent moiety of FAcCPan or FAcOPan is bound. The negatively charged carboxylic oxygen moieties of the ligands and the fluorine in the case of FAc are usually in contact with Thr^{42}-N and/or Gly^{69}-N in a seemingly random manner in terms of hydrogen bond donor-acceptor matching, suggesting that the backbone amide groups of Thr^{42} and Gly^{69} may be crucial binding interactions available at the active site to bind the substrate.

Computational Docking of FAcCoA to FlK—We have modeled a FAcCoA molecule into WtFlK (Fig. 5), based on the crystal structures of FlK in complex with various ligands, especially with AcCoA. The minimum energy was calculated using the SYBYL 8.1.1.09097 program. In a similar way to the AcCoA bound in T42SFlK, the 3′-phosphoryl-ADP region of the docked FAcCoA is at the enzyme surface in front of the entrance of the tunnel leading to the active site. The rest of the molecule extends into the tunnel, where the pantetheinyl moiety interacts through its N_{12}, O_9, N_{14}, and C_{19}, respectively, with the main chain oxygen and the side chain of His^{76}, Ala^{79}-N, and Phe^{128}-$C_{\epsilon 1}$. The hydrogen bond between the side chains of Arg^{120} and Glu^{50} is broken due to the flip of the carboxyl group of the Glu^{50}. The fluorine is placed at a hydrogen bonding distance from Gly^{69}-N and the guanidinium group of Arg^{120}. Mutation of the Arg^{120} to Ala^{120} yielded a completely insoluble protein (data not shown), consistent with the involvement of Arg^{120} in maintaining the conformation of FlK. Thr^{42}-Oγ is now located closer (3.79 Å) to the thioester carbonyl carbon and at a better, although not optimal, position for a possible nucleophilic attack. The Thr^{42}-N that is close (2.81 Å) to the thioester carbonyl oxygen could act as an oxyanion hole for stabilization of the tetrahedral acyl-enzyme intermediate (Fig. 5).

Increased Flexibility at the Active Site Resulting from Mutations of Thr^{42}—The hydrophobic interactions between Thr^{42}-$C_{\gamma 2}$ and Ile^{72}-$C_{\gamma 2}$ in the adjacent protomer provide a "dry" environment around the catalytic $O_{\gamma 1}$ of Thr^{42}, protecting it from attacks by solvent molecules, a feature observed for other enzymes that have similar catalytic triad mechanisms (37). The Thr^{42}-$C_{\gamma 2}$ may also restrain the freedom of the substrate in the active site. Loss of this restraint imposed by the $C_{\gamma 2}$ in the T42S mutant may allow random misbinding of the substrate, which in turn may result in the substrate inhibition observed in the enzyme assays. In support of this notion, the imidazole group of the His^{76} in the complex T42AFlK·FAc has a rotational disorder of ~90° or exists in two alternative conformers not observed in WtFlK structures, and the Ser^{42} in one of the protomers of the T42SFlK·Ac structure shows a double conformation, demonstrating the increased flexibility of these residues in the absence of the Thr^{42}-$C_{\gamma 2}$ and/or -$O_{\gamma 2}$ (Fig. 6).

Conformational Change for Product Release—The positions of the main chains are almost completely conserved in all FlK structures with or without mutations and/or bound ligands. Local conformational changes, especially in the hydrophobic loop ^{33}FAEFP^{37}, are observed. The side chain conformations of Phe^{33}, Phe^{36}, and Pro^{37} in the structures with bound Ac or FAc

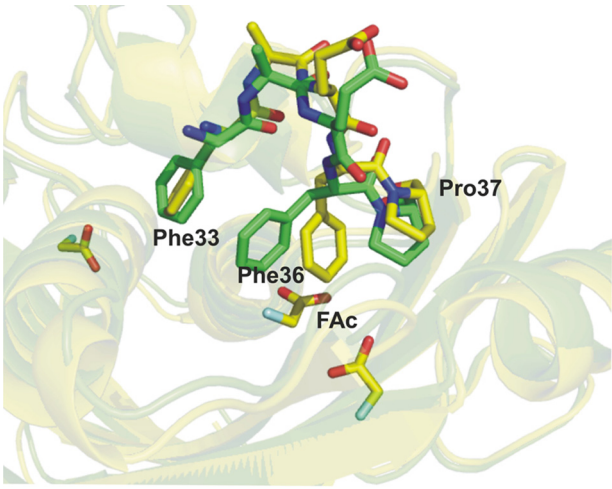

FIGURE 7. **Representation of the hydrophobic loop ^{33}FAEFP^{37} present in the active site of FlK.** Shown are the differences in the side chain for residues Phe^{33}, Phe^{36}, and Pro^{37} for WtFlK·FAc (*yellow*) and apo-WtFlK (*green*).

differ from those of unbound WtFlK and the structures in complex with AcCoA, FAcCPan, or FAcOPan (Fig. 7). In the unbound WtFlK, the planes of the phenyl rings of Phe^{33} and Phe^{36} are nearly perpendicular to each other resembling a closed two-door gate blocking the "exit" surrounded by the major helix (the "sausage"), the β-sheet (the "bun"), and the ^{33}FAEFP^{37} loop. Binding of the substrate analogues, AcCoA, FAcCPan, or FAcOPan, does not lead to any significant change in the positions of the "doors." When the active site is occupied by the product FAc or its analogue Ac, the "gate" in one of the protomers is wide open mainly due to a dramatic swing and flip of the side chain of Phe^{36}, and the gate in the other protomer of the same dimer is also open although to a lesser extent. It is tempting to speculate that this opened gate is the exit for the product FAc. The negatively charged carboxyl group of Glu^{50}, which has been "freed" from the hydrogen bond with the Arg^{120} side chain due to substrate binding, is located near the gate and may facilitate expulsion of the negatively charged FAc from the active site.

DISCUSSION

FlK, a thioesterase from fluoroacetate producing *S. cattleya*, hydrolyzes the thioester bond of FAcCoA but not that of AcCoA. The selectivity of FlK to distinguish FAcCoA from AcCoA is remarkable because it ensures that AcCoA, a key intermediate of the primary metabolism is not cleaved by mistake. The only difference between the two compounds is the presence of a fluorine atom in FAcCoA but not in AcCoA. A combination of x-ray crystallography with site-directed mutagenesis experiments allowed us to gain insights into both catalytic mechanism and the unique substrate specificity of FlK.

Our investigations suggest that FlK utilizes a catalytic triad composed of a threonine (Thr^{42}), a histidine (His^{76}), and a water molecule. The imidazole side chain of His^{76} acts as a base to deprotonate the hydroxyl of Thr^{42}. The nucleophile Thr^{42}-O$_\gamma$ attacks the fluoroacetyl carbonyl carbon, forming a tetrahedral transition intermediate. The positive charge generated on the His^{76} residue is stabilized by the hydrogen bonding between the imidazole ring and the conserved water molecule. Reformation of the carbonyl double bond breaks the carbon-sulfur bond. A second tetrahedral intermediate is then formed between the -OH part of a water molecule and the carbonyl group of the fluoroacetyl-FlK intermediate. The remaining proton of the water is bonded to His^{76}. When the carbonyl bond reforms, the bond to the Thr^{42}-O$_\gamma$ is broken, releasing the fluoroacetate. The His^{76}-bonded hydrogen is transferred to Thr^{42}-O$_\gamma$, reestablishing the hydrogen bonding between Thr^{42} and His^{76}. The Glu^{50}, which is conserved in most type II thioesterases as the catalytic residue, is not a part of the catalytic mechanism of FlK but plays an important role in maintaining the configuration of the active site.

It is not unexpected that T42SFlK is active because the Ser^{42}-Oγ can still form a hydrogen bond with the imidazole side chain of His^{76} and therefore has the potential to act as a nucleophile as the Thr^{42}-O$_\gamma$ in WtFlK. When FAcCoA concentration was higher than 12 μM, however, excess-substrate inhibition (38) was observed for the mutant. In other words, high concentrations of FAcCoA inhibited the activity of T42SFlK. We speculate that the absence of the Thr^{42}-C$_\gamma$ in T42SFlK may have created more space, allowing an easier access of substrate to the active site, especially at low substrate concentrations, giving rise to the lower K_m value and the higher turnover of T42SFlK reaction as compared with WtFlK activity. However, the same mutation also increased protein flexibility, as shown by the double confirmations of the active site residues in some of the protomers of the mutant (Fig. 6). The enzyme-substrate complex formed between these abnormal active sites and substrate could be non-productive. At high substrate concentrations, the chance of non-productive enzyme-substrate complex formation increases when more and more normal active sites are occupied by FAcCoA. The formation of non-productive enzyme-substrate complex at the active site of one protomer may also interfere with the catalytic activity of the partner protomer of the same dimer. These may explain the excess-substrate inhibition phenomenon observed for T42SFlK and E50AFlK, but the exact mechanism remains to be elucidated.

FlK is a homodimer with a hot dog fold similar to other type II thioesterases, although it does not show extensive sequence similarity to any type II thioesterases with known function. A common feature shared by nearly all functionally characterized hot dog fold thioesterases is the presence of an acidic residue, aspartate or glutamate, providing general base catalysis. One exception is FcoT, a long-chain fatty acyl-CoA thioesterase from *Mycobacterium tuberculosis*, which has a hot dog fold but uses an active site completely different from that of either type I or type II thioesterases. FcoT has been proposed to represent a new class of thioesterases, type III thioesterases (39). With a type II thioesterase fold, the catalytic machinery of FlK (Thr-His-water) resembles those of type I thioesterases (Ser/Cys-base-acid), exhibiting an unconventional combination of protein fold and catalytic mechanism. Superposition of FlK with 18 structures of type II thioesterases from the Protein Data Bank reveals that the Glu^{50} in FlK is well conserved in most of these thioesterases,

although in some cases, it is an aspartate instead of a glutamate (data not shown).

Among all of the hot dog fold proteins in the Protein Data Bank, only two hypothetical proteins, TTHA0967 (Protein Data Bank entry 2CWZ) from *Thermus thermophilus* and TM0581 (Protein Data Bank entry 2Q78) from *Thermotoga maritime*, have shown head-to-tail sequence similarity to FlK (33 and 22% identity, respectively). Superposition of FlK with these two structures has revealed a very similar putative active site in 2CWZ and 2Q78. Most of the residues lining the active site of FlK, Thr^{42}, Glu^{50}, Gly^{69}, and His^{76}, are well conserved in 2CWZ (Thr^{36}, Glu^{44}, Gly^{63}, and His^{76}) and in 2Q78 (Thr^{38}, His^{72}, and Arg^{116}) with the following differences. First, the counterpart of the Arg^{120} of FlK in 2CWZ is a glutamine (Gln^{115}). The Arg^{120} in the unliganded FlK interacts through its guanidinium group with the carboxyl side chain of Glu^{50}. The amide side chain of Gln^{115} in CWZ2, however, is pointing in the opposite direction with no possibility of forming any direct contact with Glu^{44}. A large empty space can be observed in the putative active site of 2CWZ due to this change of Arg to Gln. If 2CWZ is also an acyl-CoA thioesterase, the substrate should have a larger acyl moiety than a fluoroacetyl group. Second, the equivalents of FlK Glu^{50} and Gly^{69} in 2Q78 are His^{46} and Val^{65}, respectively. The imidazole side chain of the His^{46} and the isopropyl group of the Val^{65} at the active site provide a binding motif quite different from that in FlK.

The significant differences in the overall positions of FAcCPan and FAcOPan in the active site of FlK as compared with that of the acetyl-pantheteinyl segment of the T42SFlK-bound AcCoA (Fig. 3) suggest that binding of the nucleotide portion of the substrate on the enzyme surface dictates the depth to which the fluoroacetyl pantetheinyl arm extends into the active site cleft, ensuring the correct interaction between the arm with the amino acid residues in the vicinity of the active site. Although the sulfur atom of the thioester is considered a poor hydrogen bond acceptor, the transient dipole interaction between the sulfur and the main chain amides along the substrate binding tunnel may also contribute to positioning of the substrate. In the absence of the bulky nucleotide tail and the sulfur atom, FAcCPan moved further into the active site. FAcOPan is retained near the tunnel entrance because the oxygen atom replacing the sulfur atom has a stronger tendency to interact with the main chain amides of the substrate binding tunnel.

Although the 3′-phosphoryl ADP tail of FAcCoA is required for the overall positioning of FAcCoA in the FlK active site, the accurate orientation of the fluoroacetyl thioester moiety must be fine tuned by the hydrogen bonding of the fluorine with the side chain of Arg^{120} and the main chain amide of Gly^{69} in order to assume the required catalytic coordination. The guanidinium group of Arg^{120} and the main chain amide of Gly^{69} appear to be the key determinants for the unusual high substrate specificity of FlK, which serve to recognize the only structural difference between FAcCoA and AcCoA through their interactions with the fluorine of FAcCoA. Moreover, the thioester carbonyl carbon in FAcCoA is more positively charged than that in AcCoA due to the strong electronegativity of fluorine. The interactions between the fluorine and Arg^{120}/Gly^{69} also help to stabilize this positive charge, making the carbonyl carbon a better target for nucleophilic attack by Thr^{42}-O_γ (Fig. 5).

Acknowledgment—We thank Dr. David O'Hagan (University of St. Andrews) for helpful discussions.

REFERENCES

1. Sanada, M., Miyano, T., Iwadare, S., Williamson, J. M., Arison, B. H., Smith, J. L., Douglas, A. W., Liesch, J. M., and Inamine, E. (1986) *J. Antibiot.* **39,** 259–265
2. O'Hagan, D., Schaffrath, C., Cobb, S. L., Hamilton, J. T., and Murphy, C. D. (2002) *Nature* **416,** 279
3. Schaffrath, C., Deng, H., and O'Hagan, D. (2003) *FEBS Lett.* **547,** 111–114
4. Deng, H., O'Hagan, D., and Schaffrath, C. (2004) *Nat. Prod. Rep.* **21,** 773–784
5. Dong, C., Huang, F., Deng, H., Schaffrath, C., Spencer, J. B., O'Hagan, D., and Naismith, J. H. (2004) *Nature* **427,** 561–565
6. Zhu, X., Robinson, D. A., McEwan, A. R., O'Hagan, D., and Naismith, J. H. (2007) *J. Am. Chem. Soc.* **129,** 13597–14604
7. Huang, F., Haydock, S. F., Spiteller, D., Mironenko, T., Li, T. L., O'Hagan, D., Leadlay, P. F., and Spencer, J. B. (2006) *Chem. Biol.* **13,** 475–484
8. Peters, R., and Wakelin, R. W. (1953) *Proc. R. Soc. Lond. B Biol. Sci.* **140,** 497–506
9. Lauble, H., Kennedy, M. C., Emptage, M. H., Beinert, H., and Stout, C. D. (1996) *Proc. Natl. Acad. Sci. U.S.A.* **93,** 13699–13703
10. Ollis, D. L., Cheah, E., Cygler, M., Dijkstra, B., Frolow, F., Franken, S. M., Harel, M., Remington, S. J., Silman, I., Schrag, J., Sussman, J. L., Verschueren, K. H. G., and Goldman, A. (1992) *Protein Eng.* **5,** 197–211
11. Pleiss, J., Fischer, M., and Schmid, R. D. (1998) *Chem. Phys. Lipids* **93,** 67–80
12. Leesong, M., Henderson, B. S., Gillig, J. R., Schwab, J. M., and Smith, J. L. (1996) *Structure* **4,** 253–264
13. Li, J., Derewenda, U., Dauter, Z., Smith, S., and Derewenda, Z. S. (2000) *Nat. Struct. Biol.* **7,** 555–559
14. Dillon, S. C., and Bateman, A. (2004) *BMC Bioinformatics* **5,** 109
15. Pidugu, L. S., Maity, K., Ramaswamy, K., Surolia, N., and Suguna, K. (2009) *BMC Struct. Biol.* **9,** 37
16. Seemüller, E., Lupas, A., Stock, D., Löwe, J., Huber, R., and Baumeister, W. (1995) *Science* **268,** 579–582
17. Otwinowski, Z., and Minor, W. (1997) *Methods Enzymol.* **276,** 307–326
18. French, G. S., and Wilson, K. S. (1978) *Acta Crystallogr. A* **34**, 517–525
19. Collaborative Computational Project 4 (1994) *Acta Crystallogr. D* **50**, 760–763
20. Leslie, A. G. (2006) *Acta Crystallogr. D* **62**, 48–57
21. Evans, P. (2006) *Acta Crystallogr. D* **62**, 72–82
22. Adams, P. D., Grosse-Kunstleve, R. W., Hung, L. W., Ioerger, T. R., McCoy, A. J., Moriarty, N. W., Read, R. J., Sacchettini, J. C., Sauter, N. K., and Terwilliger, T. C. (2002) *Acta Crystallogr. D* **58**, 1948–1954
23. Navaza, J. (2001) *Acta Crystallogr. D* **57**, 1367–1372
24. Murshudov, G. N., Vagin, A. A., and Dodson, E. J. (1997) *Acta Crystallogr. D* **53**, 240–255
25. McRee, D. E. (1999) *J. Struct. Biol.* **125,** 156–165
26. Emsley, P., and Cowtan, K. (2004) *Acta Crystallogr. D* **60**, 2126–2132
27. Laskowski, R. A., MacArthur, M. W., Moss, D. S., and Thornton, J. M. (1993) *J. Appl. Crystallogr.* **26**, 283–291
28. DeLano, W. L. (2002) *The PyMOL Molecular Graphics System*, DeLano Scientific, San Carlos, CA
29. Benning, M. M., Wesenberg, G., Liu, R., Taylor, K. L., Dunaway-Mariano, D., and Holden, H. M. (1998) *J. Biol. Chem.* **273,** 33572–33579
30. Thoden, J. B., Zhuang, Z., Dunaway-Mariano, D., and Holden, H. M. (2003) *J. Biol. Chem.* **278,** 43709–43716
31. Willis, M. A., Zhuang, Z., Song, F., Howard, A., Dunaway-Mariano, D., and Herzberg, O. (2008) *Biochemistry* **47,** 2797–2805

32. Hisano, T., Tsuge, T., Fukui, T., Iwata, T., Miki, K., and Doi, Y. (2003) *J. Biol. Chem.* **278,** 617–624
33. Yokoyama, T., Choi, K. J., Bosch, A. M., and Yeo, H. J. (2009) *Biochim. Biophys. Acta* **1794,** 1073–1081
34. Kunishima, N., Asada, Y., Sugahara, M., Ishijima, J., Nodake, Y., Sugahara, M., Miyano, M., Kuramitsu, S., Yokoyama, S., and Sugahara, M. (2005) *J. Mol. Biol.* **352,** 212–228
35. Song, F., Zhuang, Z., Finci, L., Dunaway-Mariano, D., Kniewel, R., Buglino, J. A., Solorzano, V., Wu, J., and Lima, C. D. (2006) *J. Biol. Chem.* **281,** 11028–11038
36. Allaire, M., Chernaia, M. M., Malcolm, B. A., and James, M. N. (1994) *Nature* **369,** 72–76
37. Dodson, G., and Wlodawer, A. (1998) *Trends Biochem. Sci.* **23,** 347–352
38. Kühl, P. W. (1994) *Biochem. J.* **298,** 171–180
39. Wang, F., Langley, R., Gulten, G., Wang, L., and Sacchettini, J. C. (2007) *Chem. Biol.* **14,** 543–551